ChemPubSoc Europe

DOI: 10.1002/open.201800029

Open Access ChemistryOPEN Full Papers

Synthesis of Novel Aza-aromatic Curcuminoids with Improved Biological Activities towards Various Cancer Cell Lines

Atiruj Theppawong,[a] Tim Van de Walle,[a] Charlotte Grootaert,[b] Margot Bultinck,[a] Tom Desmet,[c] John Van Camp,*[b] and Matthias D'hooghe*[a]

Curcumin, a natural compound extracted from the rhizomes of *Curcuma longa*, displays pronounced anticancer properties but lacks good bioavailability and stability. In a previous study, we initiated structure modification of the curcumin scaffold by imination of the labile β-diketone moiety to produce novel β-enaminone derivatives. These compounds showed promising properties for elaborate follow-up studies. In this work, we focused on another class of nitrogen-containing curcuminoids with a similar objective: to address the bioavailability and stability issues and to improve the biological activity of curcumin. This paper thus reports on the synthesis of new pyridine-, indole-, and pyrrole-based curcumin analogues (aza-aromatic curcuminoids) and discusses their water solubility, antioxidant activity, and antiproliferative properties. In addition, multivariate statistics, including hierarchical clustering analysis and principal component analysis, were performed on a broad set of nitrogen-containing curcuminoids. Compared to their respective mother structures, that is, curcumin and bisdemethoxycurcumin, all compounds, and especially the pyridin-3-yl β-enaminone analogues, showed better water solubility profiles. Interestingly, the pyridine-, indole-, and pyrrole-based curcumin derivatives demonstrated improved biological effects in terms of mitochondrial activity impairment and protein content, in addition to comparable or decreased antioxidant properties. Overall, the biologically active *N*-alkyl β-enaminone aza-aromatic curcuminoids were shown to offer a desirable balance between good solubility and significant bioactivity.

1. Introduction

Curcumin, isolated from a local plant in Asia and also known as the golden spice, is frequently used as a food additive. Chemically, the structure of curcumin features two vanillylidene groups, keto–enol tautomerism, and a conjugated system (Figure 1), and this molecule was successfully prepared for the first time in excellent yield by Pabon in 1964.[1] In that respect, the use of boron complexed with acetylacetone was shown to produce symmetrical curcumin derivatives efficiently. Since then, several publications have described how this procedure can be to applied to prepare a diversity of related target compounds.[1,2] From a biological point of view, curcumin displays multiple activities, especially in the field of oncology.[3] Moreover, curcumin has long been considered to be an ideal compound to treat cancer due to several reports highlighting its nontoxicity for mammals, even at high doses.[4] Despite the established benefits of curcumin, it still suffers from limited bioavailability, fast metabolism in the body, and rather aspecific activity.[5] To circumvent these problems and to improve its pharmacological properties, many reported approaches focus on the introduction of structural modifications of the curcumin scaffold to deliver new analogues.[6] In that respect, previous work in our group aimed at the preparation of nitrogen curcumin analogues and involved modification of the labile β-diketone moiety by synthesizing new β-enaminone curcuminoids by using both alkylamines and more polar

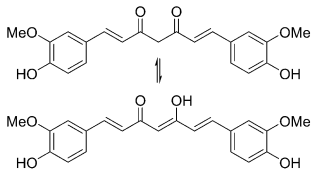

Figure 1. Structure of curcumin.

[a] *A. Theppawong, T. Van de Walle, M. Bultinck, Prof. Dr. M. D'hooghe*
SynBioC Research Group
Department of Green Chemistry and Technology
Faculty of Bioscience Engineering, Ghent University
Coupure Links 653, 9000 Ghent (Belgium)
E-mail: matthias.dhooghe@UGent.be

[b] *Dr. C. Grootaert, Prof. Dr. J. Van Camp*
Department of Food Technology, Safety and Health
Faculty of Bioscience Engineering, Ghent University
Coupure Links 653, 9000 Ghent (Belgium)
E-mail: john.vancamp@UGent.be

[c] *Prof. Dr. T. Desmet*
Department of Biotechnology
Faculty of Bioscience Engineering, Ghent University
Coupure Links 653, 9000 Ghent (Belgium)

Supporting Information and the ORCID identification number(s) for the author(s) of this article can be found under: https://doi.org/10.1002/open.201800029.

amines.[7] The obtained *N*-alkyl β-enaminones showed higher cytotoxicity than curcumin, but similar water solubility. On the other hand, more polar β-enaminone curcumin derivatives displayed significantly improved water solubility and comparable bioactivities against undifferentiated cancer cells, in addition to no toxicity against differentiated intestinal cells. The rationale to introduce a β-enaminone moiety was related to the broad biological relevance of β-enaminones in general, including for example, antimicrobial,[8] anticonvulsant,[9] and antitumor/anticancer properties.[7,10]

Up to now, the replacement of the aromatic moiety of curcumin with an azaheteroaromatic alternative—another way to introduce nitrogen—has been rarely envisaged in curcumin chemistry. Only a few isolated examples have been reported in the literature so far,[11] and these compounds are poorly documented in terms of their synthesis, characterization, physical properties, and bioactivities. Therefore, in this work, a set of new azaheteroaromatic curcumin analogues was synthesized to address the low water solubility of curcumin, without compromising its pronounced bioactivities. Because of the good results obtained previously for β-enaminone derivatives, β-enaminone aza-aromatic curcuminoids were synthesized as well by using different amines. All of these new azaheteroaromatic analogues were evaluated in a next stadium for their in vitro biological behavior, water solubility, and antioxidant capacity. Finally, multivariate statistics were performed on a broad set of nitrogen-containing curcuminoids to shed more light on structure–property relationships.

2. Results and Discussion

In this work, azaheteroaromatic curcumin analogues were successfully prepared by using carefully optimized reaction conditions (Table S1, Supporting Information). Three different aldehydes were selected to synthesize the desired structures: pyridine-3-carboxaldehyde, indole-3-carboxaldehyde, and pyrrole-2-carboxaldehyde. Boron complexation (B_2O_3) with acetylacetone (**1**) was deployed to protect the active methylene unit and to avoid the typical side reaction (i.e. formation of a C3 Knoevenagel product). The reactions were performed in ethyl acetate at 80 °C for at least 4 h and were monitored by TLC or LC–MS to reach maximum conversion. Relative to the reaction time required for bis-pyridine **2** (4 h), longer reaction times were required for bis-indole **3** (20 h) and bis-pyrrole **4** (18 h) to obtain the desired products in yields of 9 and 20%, respectively (Table S1). However, for compounds **3** and **4**, the reaction was alternatively performed in acetonitrile by using piperidine as a base, which provided improved yields of 49 and 66%, respectively (Scheme 1). To obtain the pure products, the crude mixtures were purified by silica gel column chromatography followed by recrystallization from methanol. Subsequently, bis-pyridine **2** was selected to be used in the synthesis of the corresponding β-enaminone derivatives. As established in our previous studies, the use of montmorillonite K10 (MK10), in combination with microwave irradiation, provides a convenient method to prepare β-enaminone curcuminoids.[7] Thus, the proposed imination of structure **2** was performed accordingly

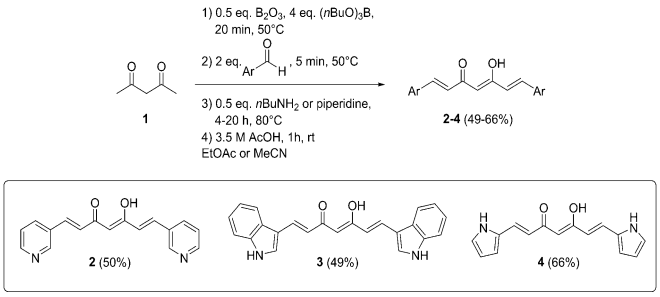

Scheme 1. Synthesis of azaheteroaromatic curcumin analogues **2**–**4**.

with either methoxyalkyl-, hydroxyalkyl-, or alkylamines (RNH_2) and 2.4 equivalents of acetic acid in the presence of MK10 (Scheme 2, Table 1). Several attempts were made to optimize the reaction conditions towards the synthesis of β-enaminone pyridin-3-yl curcumin analogues **5a**–**f**. The reaction was conducted in 2-methyltetrahydrofuran (2-MeTHF) or ethanol at 80–85 °C for 75–105 min. Although full conversion was always reached, the amount of amine added (2.5–10 equiv) had to be optimized for each amine separately. In some cases, polar amines triggered the formation of cyclic side products (i.e. compounds **6d** and **6f**), for which the reaction mechanism is described in previous work.[7b] The ratio of β-enaminones **5d** or **5f** versus dihydropyridin-4-ones **6d** or **6f** was found to be 1.5–2.3/1 (Scheme 2). A longer reaction time (105 min) apparently stimulated this cyclization reaction, and as described before, the use of ethanol was also observed to activate pyridinone formation under microwave irradiation (Table 1).[7b]

The obtained curcuminoids were then purified by column chromatography to obtain compounds **5a**–**f**, **6d**, and **6f** in rather low yields (6–24%) but excellent purity. As can be noticed, a substantial amount of product was inevitably lost during either normal- or reverse-phase column chromatography.

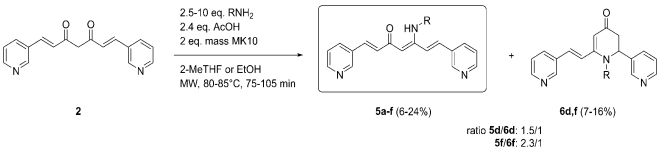

Scheme 2. Synthesis of β-enaminones **5a**–**f** and cyclic products **6d** and **6f**.

Table 1. Reaction conditions and yields for the synthesis of β-enaminones **5a**–**f** and cyclic products **6d** and **6f**.

Compd	R	RNH_2 [equiv]	*T* [°C]	Time [min]	Yield [%]
5a	*i*Bu	5	80[a]	75	24
5b	cyclohexyl	10	80[b]	90	6
5c	$(CH_2)_2OMe$	5	80[b]	75	16
5d	$(CH_2)_3OMe$	2.5	85[b]	105	24
5e	$(CH_2)_2OH$	5	80[b]	75	12
5f	$(CH_2)_3OH$	2.5	85[b]	105	16
6d	$(CH_2)_3OMe$	2.5	85[b]	105	16
6f	$(CH_2)_3OH$	2.5	85[b]	105	7

[a] Using 2-MeTHF. [b] Using EtOH.

With the aim to improve the water solubility and bioactivity and to extend the available compound library, new azaheteroaromatic curcumin analogues **2**–**4**, β-enaminone analogues **5a**–**f**, and dihydropyridin-4-ones **6d** and **6f** were thus produced in this work. All compounds had a purity of ≥95%, which was determined by NMR spectroscopy and LC–MS analysis. Afterwards, these molecules were examined in terms of their water solubility to support the rationale of this work. The main reason behind the applied structure modification was to improve the solubility and hence to avoid in vitro precipitation of compound dilutions and more specifically to increase their bioaccessibility (because higher aqueous solubility usually results in better oral bioavailability). Curcuminoids may be absorbed through the gastrointestinal tract through a combination of processes including passive diffusion and active transport. In that respect, the water solubility of compounds **2**–**6** was analyzed by using a colorimetric technique-based assay at two different time points (90 min and 24 h) to make sure that the solubility values reached the maximum concentration for each compound. An excess amount of solid was dissolved in a phosphate buffer at pH 6.8 by using the shake flask method, which is commonly used to determine aqueous solubility.[7b,12] The experiments were designed for 24 h at 37 °C average body temperature. The values were obtained on the basis of linear regression of each standard curve, which was independently triplicated. The results show that the solubilities of modified compounds **2**–**6** are all higher than that of curcumin, as shown in Table 2. Specifically, aza-aromatic curcumin analogues showed a 3- to 28-fold increase in water solubility, whereas pyridine-based β-enaminone curcumin analogues **5a**–**f** demonstrated significantly improved solubility in the range of 4- to 1600-fold. Specifically, β-enaminones with polar amines displayed extremely high aqueous solubility. Moreover, compounds **6d** and **6f** showed high water solubility in buffer medium, in the same range as that of their respective β-enaminones **5d** and **5f**. These results imply that the modification successfully addressed one of the main goals of our work, which was to obtain derivatives with improved aqueous solubility.[7] Therefore, these results can contribute to minimized precipitation issues in a biological medium for anticancer evaluation, which is beneficial within the framework of bioavailability studies.

Table 2. Determination of solubility experiments in 0.1 M phosphate buffer pH 6.8 and evaluation of chemical antioxidant capacity using FRAP assays.[a]

Compd	Solubility in 0.1 M phosphate buffer pH 6.8 [μM]		FRAP [Trolox equiv per μM]
	90 min	24 h	
curcumin	2.9 ± 0.3	2.60 ± 0.0	1.11
α-tocopherol	–	–	0.76
Trolox	–	–	–
2	12.4 ± 0.2	9.2 ± 0.1	0.03
3	19.0 ± 0.2	11.1 ± 0.1	0.27
4	84.8 ± 2.8	74.2 ± 1.3	0.79
5a	168.4 ± 6.0	303.0 ± 16.0	0.03
5b	11.3 ± 0.6	12.2 ± 0.6	0.00
5c	895.0 ± 18.0	2282.5 ± 174.0	0.00
5d	897.4 ± 1.1	2313.5 ± 90.0	0.01
5e	4350.8 ± 260.0	4847.2 ± 140.0	0.04
5f	1472.8 ± 24.0	4270.5 ± 332.0	0.04
6d	1283.1 ± 61.2	2981.7 ± 165.8	0.00
6f	2462.6 ± 57.2	4999.0 ± 136.8	0.00

[a] $n = 3$ triplicate independent experiments.

Because curcumin is known to exert interesting antioxidant activities, the antioxidant properties of the newly synthesized azaheteroaromatic curcumin analogues were determined by using the DPPH (1,1-diphenyl-2-picrylhydrazyl) radical-scavenging activity assay and the ferric reducing antioxidant power (FRAP) assay.[13] Trolox and α-tocopherol were used as antioxidant positive controls (for the DPPH and FRAP assays, respectively). The DPPH and FRAP assays are commonly used primarily to evaluate the chemical antioxidant properties. The DPPH scavenger assay is based on the neutralization of the stable DPPH radical and determines the percentage inhibition of radical activity. On the other hand, the FRAP assay is based on the reduction of the ferric(III)–tripyridyltriazine complex (Fe^{3+}–TPTZ) to the ferrous form (Fe^{2+}–TPTZ) and is expressed as Trolox equivalents. The results of the chemical antioxidant capacity tests are described in Table 1. From all aza-aromatic curcumins, bis-pyridine **2** showed no activity, whereas compounds **3** and **4** could not be evaluated by the DPPH assay due to the saturation of the selected wavelength ($\lambda = 515$ nm) for this experiment (see the Supporting Information). Therefore, an alternative method was deployed (using FRAP), and bis-pyrrole **4** (0.79 Trolox equivalent per μM) showed activity comparable to that of α-tocopherol, whereas bis-indole **3** (0.27 Trolox equivalent per μM) showed antioxidant properties that were lower than those of the controls. This could be explained by the fact that the free NH functionality on the azaheteroaromatic ring can be equipotent to the hydroxy groups in the curcumin scaffold. Compounds **5** and **6** showed no/lower antioxidant activity than curcumin and the positive controls, probably because these structures do not contain a hydroxy group on the pyridinyl curcumin core. Compounds **5e** and **5f**, containing a hydroxy moiety in the β-enaminone nitrogen substituent, showed slightly lower activity upon the FRAP experiment (0.04 Trolox equivalent per μM), whereas the median effective concentration (EC_{50}) values under the highest concentration (200 μM) could not be observed as explicitly upon performing the DPPH experiment. The lack of phenolic groups (due to the replacement of the aromatic part of curcumin with a pyridin-3-yl scaffold) resulted in complete abolition of the antioxidant activity in both assays, which further supports the established importance of the free phenolic (or amino) groups if antioxidant properties are desired.

Next to these antioxidant properties, curcuminoids have shown a wide range of other biological activities, in particular anticancer effects.[3b,d,f,14] Therefore, different cell lines were subjected to newly synthesized nitrogen curcuminoids **2**–**6** and were analyzed through in vitro cell-based assays for protein content as a marker for cell growth (sulforhodamine B, SRB), mitochondria activity [3-(4,5-dimethylthiazol-2-yl)-2,5-diphenyltetrazolium bromide, MTT], and intracellular reactive oxygen species (ROS) production (2′,7′-dichlorodihydrofluores-

Table 3. Cell growth inhibition of **2**–**4**, **5a**–**f**, **6a**, and **6b** measured after 72 h treatment by using mitochondria activity (MTT) and protein content (SRB) assays.[a]

Compd	Caco-2 IC_{50} [μM]		EA.hy926 IC_{50} [μM]		HT-29 IC_{50} [μM]		HepG2 IC_{50} [μM]		CHO-K1 IC_{50} [μM]	
	MTT	SRB	MTT	SRB	MTT	SRB	MTT	SRB	MTT	SRB
Cur	28.0±6.4	33.1±4.5	20.0±5.9	34.7±10.5	23.4±5.1	20.3±1.1	20.3±4.1	21.3±4.0	21.3±8.9	33.5±2.3
Dox	11.1±1.0	12.1±0.8	1.4±0.5	1.4±0.3	4.0±0.9	3.5±0.4	5.5±1.4	2.5±1.2	1.4±0.5	6.2±1.7
N-acetyl-L-cysteine	>75	>75	–	–	–	–	–	–	–	–
2	6.9±2.5	7.3±3.1	7.9±1.9	11.2±2.8	8.2±0.8	6.1±3.4	8.3±0.7	10.0±1.6	7.2±0.3	10.5±2.1
3	3.3±0.3	2.1±0.6	11.7±4.6	15.2±5.9	11.5±6.7	15.3±6.6	10.0±1.7	10.4±1.5	7.9±1.3	12.1±5.6
4	7.5±1.6	9.7±0.6	8.3±0.9	9.0±2.2	8.9±0.5	9.6±0.5	8.2±0.9	9.8±1.5	6.9±3.0	11.7±2.7
5a	45.3±10.5	31.6±9.0	33.0±9.5	35.9±7.2	37.6±1.8	30.9±10.9	26.2±0.3	20.8±1.5	17.7±4.4	28.6±7.7
5b	65.6±2.1	60.8±6.0	40.2±1.4	53.0±1.9	36.4±7.9	19.4±0.9	>75	>75	16.8±1.1	20.4±0.6
5c	53.8±0.6	49.1±0.6	60.0±10.5	63.0±8.3	55.3±12.5	46.0±15.8	56.7±3.7	66.4±1.3	45.1±6.6	71.7±5.1
5d	28.5±3.5	36.0±0.1	70.6±2.5	72.7±3.7	59.6±7.7	51.5±6.1	>75	>75	21.3±3.7	24.1±1.7
5e	>75	>75	>75	>75	>75	>75	>75	>75	>75	>75
5f	>75	>75	>75	>75	>75	>75	>75	>75	>75	>75
6d	>75	>75	>75	>75	>75	>75	>75	>75	>75	>75
6f	>75	>75	>75	>75	>75	>75	>75	>75	>75	>75

[a] Data are presented as mean ± standard deviation. Combination data of MTT and SRB from two different students on curcumin analogues ($n \geq 6$).

cein diacetate, DCFH-DA) to evaluate their cytotoxic effects. Cancer cell lines included human-derived intestinal cells (HT-29 and Caco-2), endothelial cells (EA.hy926), a hepatoma cell line (HepG2), and a Chinese hamster ovarian cell line (CHO-K1). Doxorubicin was used as a positive control for MTT and SRB experiments, whereas in the ROS experiments, the ROS inhibitor *N*-acetyl-L-cysteine (NAC) was used as experiment control. The IC_{50} values obtained through MTT and SRB are shown in Table 3. Based on the observations made, different cell lines resulted in different median inhibitory concentration (IC_{50}) values, strongly depending on the cell type. Interestingly, aza-aromatics **2**–**4** showed higher mitochondrial activity/growth inhibition (MTT) than their mother compound curcumin. To support these results, a protein content experiment (SRB) was then performed, and the results pointed to the same trend as that observed for the MTT assay, which confirmed that azaheteroaromatic analogues **2**, **3**, and **4** exhibit significantly stronger cell growth inhibition effects than curcumin. On the other hand, β-enaminones **5a**–**d** demonstrated moderate growth inhibition, whereas **5e** and **5f** showed no activity at maximum concentration (75 μM). In terms of their water solubility, β-enaminones **5a**–**f** performed better than azaheteroaromatic analogues **2**–**4** and curcumin. No solids were observed after an incubation time of 72 h for the MTT and SRB assays for compounds **5a**–**f**. Thus, it seems that the more soluble compounds exert decreased cytotoxicity due to a low cell membrane permeability effect, which will be elaborated further on. Moreover, dihydropyridin-4-ones **6d** and **6f** showed a trend similar to that shown by **5e** and **5f** concerning their bioactivity and water solubility. Thus, the aim to improve water solubility was successfully reached for all structures, whereas the bioactivity towards cancer cells was slightly lower for β-enaminones **5a**–**f** and considerably higher for aza-aromatics **2**–**4**. In contrast, dihydropyridin-4-ones **6d** and **6f** showed no interesting cytotoxicity, pointing to the importance of conserving the linear curcumin scaffold if cancer cell proliferation is targeted. Thus, the introduction of a nitrogen atom in the aromatic moiety of the curcumin scaffold has a positive influence on the antiproliferative properties of curcumin, provided that the conjugated curcumin structure remains intact. Although azaheteroaromatic β-enaminones **5a**–**f**, especially the most polar ones, show slightly lower (yet still significant) cytotoxic effects than non-β-enaminone template compound **2**, the installation of a β-enaminone moiety is desired, because this increases the stability of the curcumin scaffold.[7b,15] In other words, further optimization of this class could focus on minor modifications of the nitrogen side chain to arrive at compounds with even better bioactivity, water solubility, and stability. Within our series of six azaheteroaromatic β-enaminone derivatives, compound **5a** demonstrated the highest antiproliferative activity—almost comparable to the activity of curcumin—and will therefore be used as a lead compound for the synthesis of new β-enaminones in future work.

In the next set of experiments, intracellular ROS was assessed in different cell lines because of their possible role in cytotoxicity-related pathways. The imbalance between ROS and antioxidant levels could lead to the development of cell damage and health issues, including chronic diseases.[16] Higher ROS levels are considered as toxic and sequentially cause DNA damage and, therefore, increase the risk in the first stage of cancer development.[17] Moreover, high ROS production may also cause cell apoptosis by stimulation of the intrinsic mitochondrial pathway, which induces outer membrane permeabilization and releases apoptotic proteins.[18] An antioxidant diet, rich in polyphenols, can trigger a reduction in the amount of ROS produced, which is consequently beneficial for treating several human diseases, including neurodegenerative diseases,[19] aging,[20] inflammatory injuries,[21] and cancer.[22] It is worth considering whether the observed cytotoxicity of curcuminoids may be correlated to the induction of intrinsic mitochondrial pathways by high ROS production. It is possible that the α,β-unsaturated ketone moiety can serve as a biological Michael acceptor that covalently binds to the thiol residues (SH) of cysteine compartments in different proteins and initially

triggers cascade signaling apoptosis pathways.[23] To study the impact of novel derivatives **2**–**6**, a fluorescent-based technique was conducted by using DCFH-DA, which is commonly used as a probe for oxidative stress. In this work, two concentrations of curcuminoids were tested, 10 (high) and 1 μM (mild), and they parallel plasma concentrations of curcumin in a previous study.[24] Moreover, ROS experiment results were analyzed in correlation to protein content (SRB) to normalize the ROS production values, as formerly observed MTT and SRB values showed that some IC_{50} values were lower than 10 μM. Moreover, as previously reported, the ROS response in the EA.hy926 cell line was pro-oxidative,[7a] whereas for intestinal cell lines (Caco-2 and HT-29), intracellular ROS response was decreased in some cases. In both HepG2 and CHO-K1, some compounds had an antioxidative effect.[7] In this study, at 10 μM treatment, aza-aromatics **2**–**4** all showed a strong response (intracellular ROS products) in the five different cancer cells, whereas at 1 μM, bis-indole **3** demonstrated increased ROS production in two different cell lines, HT-29 and HepG2. Moreover, bis-pyrrole **4** exhibited a trend similar to that exhibited by compound **3** but on different cells, Caco-2 and EAhy926, whereas decreased ROS generation was observed in HepG2 (indicating an antioxidant effect). For β-enaminones **5a**–**f**, the increase/decrease in ROS depended on the cell type. In Caco-2, compounds **5a**–**e** showed moderate to high ROS generation at 10 μM, whereas no increase/decrease in ROS production could be noticed at 1 μM. In contrast, in EAhy.926 and CHO-K1 cells, the ROS response slightly decreased upon applying **5a**–**c**, **5e**, and **5f** independently at 1 μM. Moreover, HT-29 and HepG2 cells, at 10 μM, were observed to provoke an antioxidant effect that minimized ROS production for **5a**–**c**, **5e**, and **f**. For dihydropyridin-4-ones **6d** and **6f**, ROS production was not remarkably visible in five different cell lines at both concentrations relative to that observed for nontreated cells. A control in these experiments was NAC, a ROS inhibitor,[25] which induced a significant decrease in ROS generation in the intestinal cell lines (Caco-2 and HT-29), the endothelial cell line (EA.hy926), and the hepatoma cell line (HepG2). An increase was only observed in CHO-K1 cells, as shown in Table 4. It is often difficult to compare results with other studies because of the different parameters used in the experimental procedures, such as cell line types, molecules, concentrations, and incubation periods.[26] To our interpretation, increased cellular ROS was observed at a 10 μM concentration for bis-indole **3** and bis-pyrrole **4** in five different cell lines, whereas bis-pyridine **2** showed a trend similar to that of the other two aza-aromatic curcuminoids, except in HepG2 cells. The reason behind the different results in HepG2 cells may be related to their robustness and detoxification mechanisms.[27] Moreover, β-enaminones **5a**–**f** showed increased cellular ROS in Caco-2 at 10 μM, whereas other cell lines were observed to display either decreased cellular ROS or no difference relative to nontreated cells (control). At 10 μM, compounds **5c**, **5d**, and **5f** exhibited significantly decreased ROS in HepG2 cells, whereas compounds **5a**–**c** showed decreased ROS in HT-29 cells. At 1 μM, in EA.hy926, decreased ROS generation was observed in **5b**, **5c**, and **5f**, whereas in compounds **5a**–**c**, **5e**, and **5f** it was observed in CHO-K1 cells. However, dihydropyridin-4-ones **6d** and **6f** showed no activity at both test concentrations (10 and 1 μM). Therefore, our results remarkably demonstrate the pro-oxidative effect of aza-aromatic curcumin analogues **2**–**4**, whereas β-enaminones **5a**–**f** show both pro-oxidative and antioxidative effects depending on the cell types. It can be concluded that there might be a correlation between the cytotoxicity effects of aza-aromatics **2**–**4** and overproduction of ROS, which was preliminary observed in MTT and SRB, suggesting that these compounds induce cytotoxic effects through ROS-mediated apoptosis pathways. Nonetheless, in the case of β-enaminones **5a**–**f** and dihydropyridin-4-ones **6d** and **6f**, no explicit link can be noted between cell viability and pro- or antioxidant activities, and other pathways might be in play as well. In these cases, the increased/decreased intracellular ROS levels were strongly cell line/compound specific.

To allow a more thorough interpretation of the results obtained by screening of the β-enaminone analogues and dihy-

Table 4. Intracellular ROS, expressed as percentage compared to the untreated control cells ($n \geq 3$) with protein content normalization (ROS/SRB).[a]

Compd	Caco-2		EA.hy926		HT-29		HepG2		CHO-K1	
	10 μM	1 μM	10 μM	1 μM	10 μM	1 μM	10 μM	1 μM	10 μM	1 μM
Cur	95.8 ± 2.5	96.7 ± 5.8	103.9 ± 7.6	99.9 ± 6.4	90.2 ± 6.1[b]	92.8 ± 5.8[b]	84.2 ± 8.1[b]	95.9 ± 13.8	91.9 ± 5.2[b]	88.7 ± 16.2
N-acetyl-L-cysteine	47.8 ± 2.6[c]	55.7 ± 5.8[c]	79.6 ± 7.4[b]	79.6 ± 11.1[b]	87.7 ± 3.7[b]	90.1 ± 12.0[b]	70.5 ± 3.1[c]	73.1 ± 2.7[b]	102.2 ± 5.4	102.4 ± 0.8
2	142.7 ± 11.9[b]	104.8 ± 15.1	116.1 ± 3.3[b]	111.5 ± 1.6[b]	127.0 ± 7.9[b]	94.0 ± 4.0	90.4 ± 11.9	99.0 ± 4.6	110.5 ± 4.5[b]	100.8 ± 4.3
3	110.3 ± 6.5[b]	95.7 ± 7.3	217.8 ± 20.3[b]	110.6 ± 7.5	125.2 ± 12.0[b]	141.4 ± 21.3[b]	382.2 ± 34.0[c]	129.1 ± 8.0[c]	109.1 ± 4.9[b]	96.4 ± 2.6
4	124.3 ± 8.7[c]	110.2 ± 9.5[b]	165.1 ± 18.9[b]	295.2 ± 38.5[c]	120.7 ± 8.7[b]	104.6 ± 6.3	120.9 ± 26.1	75.6 ± 14.6[b]	116.7 ± 4.9[b]	101.6 ± 4.9
5a	114.7 ± 3.1[b]	109.8 ± 7.4	93.4 ± 14.6	88.7 ± 9.3	84.1 ± 2.5[b]	102.9 ± 11.1	94.0 ± 4.6	90.7 ± 13.7	85.5 ± 2.6[c]	83.8 ± 4.7[b]
5b	117.7 ± 5.6[b]	101.3 ± 0.9	113.9 ± 9.5	89.1 ± 4.2[b]	90.6 ± 2.8[b]	93.7 ± 13.2	98.8 ± 4.6	92.3 ± 7.8	90.5 ± 2.5[b]	78.4 ± 3.3[c]
5c	243.2 ± 17.5[b]	102.4 ± 8.8	89.5 ± 2.7[b]	83.7 ± 6.7[b]	88.1 ± 3.6[b]	100.2 ± 5.8	88.4 ± 5.3[b]	94.8 ± 4.0	96.2 ± 10.1	84.1 ± 6.5[b]
5d	110.6 ± 5.3[b]	101.5 ± 9.2	98.3 ± 2.0	101.6 ± 5.8	95.1 ± 14.0	102.5 ± 19.4	89.4 ± 3.1[b]	92.3 ± 4.6	97.2 ± 3.9	98.0 ± 0.1
5e	118.6 ± 2.8[c]	111.4 ± 8.9	115.3 ± 7.6	101.5 ± 1.6	109.8 ± 3.7	93.9 ± 5.5	92.1 ± 5.1	88.6 ± 15.2	91.8 ± 5.6	82.2 ± 2.9[c]
5f	115.4 ± 8.5	102.5 ± 2.3	101.5 ± 1.6	88.7 ± 1.6[c]	96.0 ± 12.7	95.4 ± 1.7	74.4 ± 3.2[c]	84.8 ± 2.5[b]	86.9 ± 9.4	80.5 ± 2.8[c]
6d	89.9 ± 3.4	90.8 ± 6.3	98.3 ± 5.3	95.2 ± 5.0	88.4 ± 4.1	83.4 ± 5.6	95.7 ± 10.0	85.6 ± 8.9	103.8 ± 8.1	105.4 ± 3.4
6f	95.4 ± 9.0	100.5 ± 2.4	106.1 ± 9.9	100.6 ± 1.3	106.2 ± 4.1	111.1 ± 8.1	106.5 ± 13.1	88.8 ± 10.4	98.5 ± 5.2	91.7 ± 5.9

[a] Data are presented as mean ± standard deviation; $n \geq 3$. [b] $p < 0.05$, [c] $p < 0.001$ indicate significant increases or decreases compared to the untreated control cells according to a two-tailed student *t*-test with unequal variances.

dropyridin-4-ones (produced during current and previous studies),[7] multivariate statistics including hierarchical clustering analysis (Figure S2) and principal component analysis were used to find correlations between the chemical structures and biological activities and to suggest suitable side chains for good antiproliferative activity.[28] These analyses were applied to curcumin (Cur), bisdemethoxycurcumin (Bis), pyridin-3-yl curcuminoid **2**, and acetylated curcumin as the mother compounds for β-enaminones and dihydropyridin-4-ones (32 derivatives, Figure 2a). The multivariate statistics were computationally performed using the SPSS program (version 24).[29] To gather more information, principal component analysis (PCA) was performed to reveal the structural features of their activity. Thus, a factorial analysis (PCA) was also performed in SPSS statistics. It was observed that the two major principle components explained 46% of the variance between the different compounds. If the variables are displayed in a 2D plot based on these two principal components, we can see that three clusters are formed. Cluster 1 contains antioxidant activity and ROS activity for the CHO-K1 and EA.hy926 cell lines. Cluster 2 consists of the MTT data of all cell lines, and cluster 3 contains water solubility and ROS data of the intestinal Caco-2 and HT-29 cell lines. On the basis of these results, we may suggest that the biological behavior of the curcuminoids is mainly driven by water solubility (PCA1, 30.6% of variance) and (anti-) oxidant activity (PCA2, 15.9% of variance). Secondly, whereas the MTT data are similar between cell lines, clear cell line dependent behavior is visible for the intracellular antioxidant capacity, because the ROS data for intestinal and nonintestinal cells are positioned in opposite fields along the PCA1 axis, which may correspond with water solubility. We hypothesize that for nonintestinal cell lines, PCA1 (corresponding with solubility) determines the anticancer activity because viability (MTT) and ROS are in two opposite fields in the plot along the PCA1 axis. On the basis of existing literature, this may be explained by the absorption characteristics of the compound, which may be dominated by passive diffusion,[30] as hydrophobic compounds are more absorbed through the cell membrane. However, for intestinal cell lines, it is PCA2 (corresponding with the antioxidant activity of the compounds) that triggers the anticancer effect because viability and ROS are positioned in opposite fields along this axis. This can be explained by the fact that intestinal cells are quite robust and have a diversity in transporters for phenolics,[31] so that hydrophobicity is not exclusively necessary for bioavailability. If the compounds are displayed in a 2D plot based on these two princi-

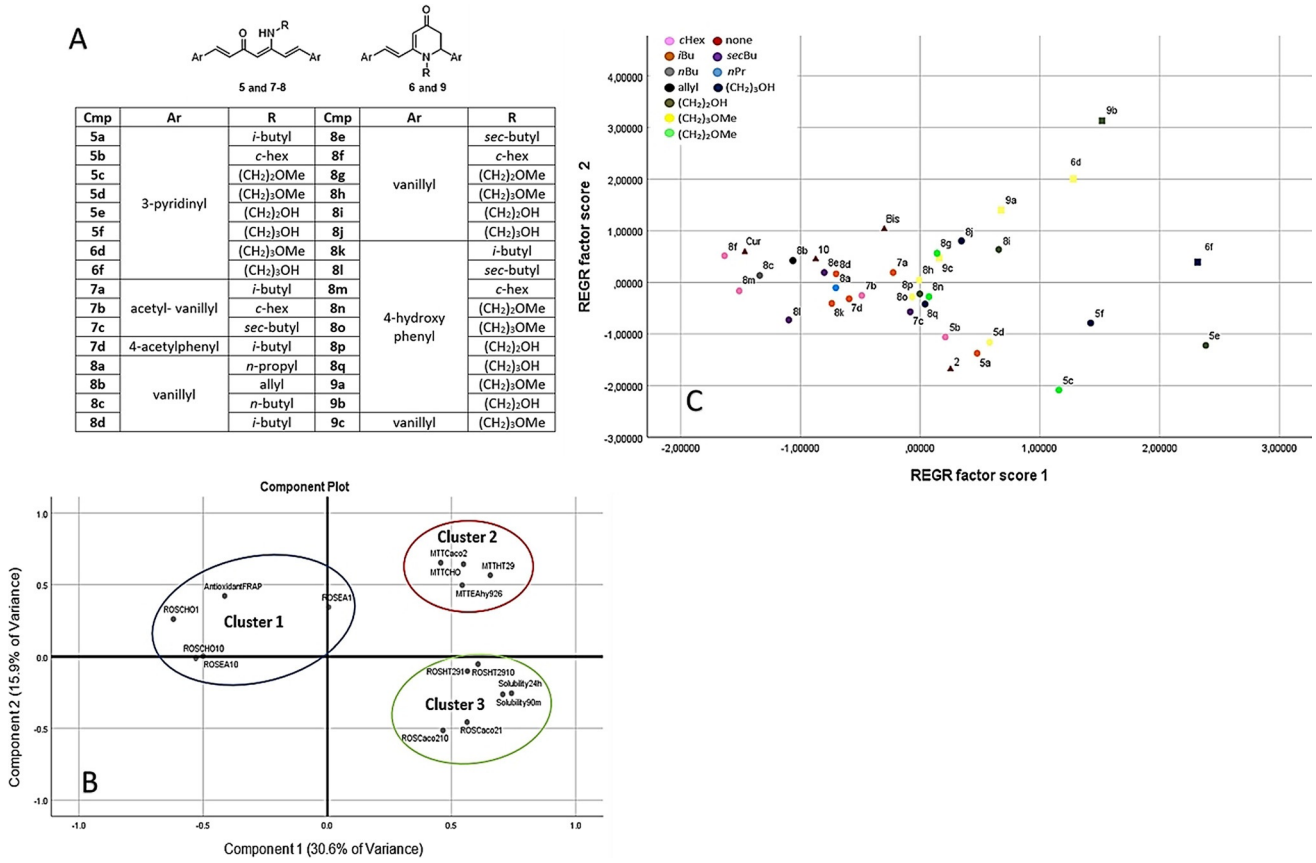

Cmp	Ar	R	Cmp	Ar	R
5a	3-pyridinyl	*i*-butyl	8e	vanillyl	*sec*-butyl
5b		*c*-hex	8f		*c*-hex
5c		$(CH_2)_2OMe$	8g		$(CH_2)_2OMe$
5d		$(CH_2)_3OMe$	8h		$(CH_2)_3OMe$
5e		$(CH_2)_2OH$	8i		$(CH_2)_2OH$
5f		$(CH_2)_3OH$	8j		$(CH_2)_3OH$
6d		$(CH_2)_3OMe$	8k	4-hydroxy phenyl	*i*-butyl
6f		$(CH_2)_3OH$	8l		*sec*-butyl
7a	acetyl- vanillyl	*i*-butyl	8m		*c*-hex
7b		*c*-hex	8n		$(CH_2)_2OMe$
7c		*sec*-butyl	8o		$(CH_2)_3OMe$
7d	4-acetylphenyl	*i*-butyl	8p		$(CH_2)_2OH$
8a	vanillyl	*n*-propyl	8q		$(CH_2)_3OH$
8b		allyl	9a		$(CH_2)_3OMe$
8c		*n*-butyl	9b		$(CH_2)_2OH$
8d		*i*-butyl	9c	vanillyl	$(CH_2)_3OMe$

Figure 2. a) Structures of β-enaminones and dihydropyridin-4-ones **5**–**9**. b) Principle component analysis (PCA) plot based on FRAP antioxidant, solubility, the IC_{50} of the MTT assay, and ROS on the CHO, EA.hy926, HT-29, and Caco-2 cell lines. c) Factor scores based on the PCA of the FRAP antioxidant, solubility, the IC_{50} of the MTT assay, and ROS on the CHO, EA.hy926, HT-29, and Caco-2 cell lines categorized by ten different side chains on either the β-enaminones or dihydropyridin-4-ones (see structures in the Supporting Information), which are indicated by colors; triangles represent mother compounds, circles represent β-enaminones, and squares represent dihydropyridin-4-ones.

pal components, we see that PCA1 (solubility) triggers the separation of the compounds by the hydrophilicity of the side chain, as nonpolar aliphatic β-enaminones are clustered in the left space and polar aliphatic β-enaminones are clustered in the right space. Hence, these hydrophobic side chains mainly have an anticancer effect on EA.hy926 and CHO-K1 cells. For hydrophilic side chains, the effect is mainly triggered by PCA2 (antioxidant capacity) in intestinal cells. This can be explained by the presence of either a vanillyl or 4-hydroxyphenyl moiety in the targeted compounds (polar and nonpolar side chains), which contain hydroxy groups displaying antioxidant properties. To maintain the antioxidant capacity, we suggest that a compound that contains a phenolic moiety should be constructed, as it may provide better activity. On the basis of the latter plot, two possibilities to improve bioavailability or bioactivity can be proposed. The first one is that polar amines can increase water solubility, which may be linked to better/poor bioavailability (cell dependence); the second one is that alkylamines can increase cytotoxicity (low IC_{50} values), which may be linked to higher bioactivity in terms of antiproliferative effects and ROS induction. To investigate the impact of side chains and the aromatic moiety as key elements in terms of stability and water solubility improvement in biological media, we display the curcuminoids by the substituted side chains in Figure 2a,c. Compounds **5c–f**, **6d**, **6f**, **8i**, **9a**, and **9b**, substituted by either a methoxy- or hydroxyalkylamine, are clustered together in the right space (Figure 2c), generally providing high solubility and high cytotoxicity. Remarkably, cyclohexyl/isobutyl-substituted β-enaminones (**5a**, **5b**, **7b**, **8c**, **8f**, **8k**, **8l**, and **8m**) showed better activity than curcumin, with slightly improved water solubility (**5a**, **7b**, **8c**, **8f**, **8k**, **8l**, and **8m**) or better solubility (**5b**). Moreover, compounds **7a**, **7c**, **7d**, **8d**, and **8e** showed activity comparable to that of mother compounds Cur and acetylated curcumin, with moderately improved water solubility. Besides, **8a** and **8b** demonstrated bioactivity that was better than or comparable to that of curcumin (Cur). On the other hand, dihydropyridin-4-ones **6d**, **6f**, and **9a–c**, bearing polar aliphatic side chains, are distributed in the right space (PCA1, solubility) without exhibiting any activity relative to their mother compounds (Cur, Bis, and **2**). Moreover, β-enaminones **5c–f**, **8g–j**, and **8o--q**, bearing polar aliphatic side chains, showed moderate to good water solubility with either comparable or lower activity. This information could suggest that alkyl side chains (*n*-propyl, *n*-butyl, allyl, isobutyl, *sec*-butyl, and cyclohexyl), as demonstrated in our β-enaminone research,[7] could be of benefit for further investigation of curcumin by using a similar platform. The improvement in water solubility is an important factor to address the classical problem of curcumin, but compounds that show high solubility could have compromised biological activity. This could imply that polar β-enaminones cannot pass the hydrophobic cell membrane of intestinal cells, thereby leading to low cytotoxicity.[32] Nevertheless, β-enaminone analogues display improved compound stability, which addresses another problem related to curcumin.

3. Conclusions

In summary, we successfully synthesized **2–4** as three new (pyridine-, indole-, and pyrrole-based) azaheteroaromatic curcumin analogues and **5a–f** as six novel azaheteroaromatic β-enaminones. To obtain pyridine β-enaminone analogues **5**, an optimized microwave irradiation approach was performed by using montmorillonite K10 clay. In some cases, this method also provided access to dihydropyridin-4-ones **6d** and **6f** by cyclization. As expected on the basis of previous observations, the installation of the central β-enaminone moiety en route to *N*-alkyl or *N*-hydroxy/methoxyalkyl β-enaminone derivatives **5** (significantly) increased the water solubility relative to that of the parent compound. Moreover, the water solubility of azaheteroaromatic curcumin derivatives **2–4** was also slightly increased relative to that of curcumin. Biologically, three new aza-aromatic curcumin derivatives (i.e. compounds **2–4**), six β-enaminones (i.e. compounds **5a–f**), and two dihydropyridin-4-ones (i.e. compounds **6d** and **6f**) were evaluated for their intracellular and chemical antioxidant properties and their cytotoxicity. Bis-indole **3** and bis-pyrrole **4** showed moderate antioxidant properties compared to curcumin (according to the ferric reducing antioxidant power assay), whereas bis-pyridine **2** did not. Cell-based experiments were performed by using five different cancer cell lines (HepG2, EA.hy926, Caco-2, HT-29, and CHO-K1). With regard to the mitochondrial activity and protein content, azaheteroaromatic curcumin derivatives **2–4** showed higher activity than curcumin, and in some cell lines they showed activity comparable to that of the positive control doxorubicin. New pyridine β-enaminones **5a–f** proved to have either moderate bioactivity or bioactivity comparable to that of curcumin. As a result of intracellular ROS generation, azaheteroaromatic curcumin compounds **2–4** showed a significant increase in intracellular ROS production, suggesting that these molecules may induce cytotoxic effects through ROS-mediated apoptosis pathways. On the other hand, compounds **5a–f** showed slight increases or decreases in ROS generation, whereas pyridinones **6d** and **6f** displayed no significant ROS variation compared to nontreated cells. In this work, we initiated a valuable incentive for exploring new curcumin analogues bearing different azaheteroaromatic and β-enaminone moieties that could lead to promising candidates in the framework of oxidative-related stress disease developments. Moreover, a structure–activity relationship study using multivariate statistics analysis showed that nonpolar aliphatic side chains demonstrated better activity than polar aliphatic side chains, which explicitly relates to their water solubility profiles. The highly soluble β-enaminone derivatives (bearing a polar aliphatic moiety) showed an inverted relationship concerning cytotoxicity. Therefore, on the basis of our results, we suggest that aliphatic amines (allyl, *n*-butyl, isobutyl, *sec*-butyl, *n*-propyl, cyclohexyl) should be used for further development to contribute to curcumin medicinal chemistry. Biologically active *N*-alkyl β-enaminone aza-aromatic curcuminoids thus offer a desirable balance between good solubility and significant bioactivity.

Experimental Section

Chemistry

^{1}H NMR spectra were recorded at 400 MHz (Bruker Avance III Nanobay) with $CDCl_3$, [D_6]DMSO, or [D_4]methanol as solvent. ^{13}C NMR spectra were recorded at 100.6 MHz (Bruker Avance III Nanobay) with $CDCl_3$, [D_6]DMSO, or [D_4]methanol as solvent. Low-resolution mass spectra were recorded by injection with an Agilent 1100 Series LC/MSD type SL mass spectrometer with electrospray ionization (ESI, 70 eV) and by using a mass-selective detector (quadrupole). Upon analyzing crude reaction mixtures, the mass spectrometer was preceded by a HPLC reverse-phase column with a diode array UV/Vis detector. High-resolution mass spectra were obtained with an Agilent Technologies 6210 time-of-flight mass spectrometer (TOFMS) equipped with ESI/APCI-multimode source. IR spectra were measured with a Fourier-transform infrared spectrophotometer (The IRaffinity-1S). Melting points of crystalline compounds were measured with a Kofler Bench, type WME Heizbank of Wagner & Munz. Microwave reactions were performed with a CEM Discover microwave at fixed temperature. The purity of all tested compounds was assessed by ^{1}H NMR spectroscopy and/or HPLC analysis, confirming a purity of $\geq$95%.

Representative Procedure for the Synthesis of Aza-Aromatic Curcumins 2–4

Acetylacetone (**1**; 20 mmol, 2.04 mL) was added to a solution of B_2O_3 (696 mg, 20 mmol, 1 equiv) in ethyl acetate or acetonitrile (60 mL). This mixture was stirred at 50 °C for 1 h. Then, pyridine-3-carboxaldehyde (3.75 mL, 40 mmol, 2 equiv) and tributyl borate [n(BuO)$_3$B; 6.53 mL, 40 mmol, 2 equiv] were added, and the mixture was further stirred at 50 °C for 10 min. Afterwards, either *n*-butylamine (0.99 mL, 10 mmol, 0.5 equiv) or piperidine (0.99 mL, 10 mmol, 0.5 equiv) in ethyl acetate or acetonitrile (10 mL) was added dropwise over 1 h, after which the mixture was stirred until the reaction reached maximum conversion at 80 °C, as determined by LC–MS.

For EtOAc as the solvent, after cooling to room temperature, 20% aq acetic acid (100 mL) was added, and the mixture was further stirred at room temperature for 1 h. The mixture was then washed with a saturated solution of sodium bicarbonate (3×50 mL), and the aqueous phase was extracted with ethyl acetate (2×30 mL). The combined organic phase was washed with water and then dried (magnesium sulfate), filtered, and concentrated under reduced pressure. Column chromatography (SiO_2, EtOAc/MeOH 19:1) afforded compound **2** (5.56 g, 50%). Upon using acetonitrile, boron decomplexation was first performed for 1 h followed by evaporation and washing with a saturated solution of sodium bicarbonate to quench the excess amount of acid and to obtain a dark red solid. The dark red solid was then subjected to purification by reverse-phase column chromatography (acetonitrile/water, gradient conditions from 30 to 100%) to obtain the pure compound. A similar procedure was then applied for compounds **3** and **4** by using indole-3-carboxaldehyde and pyrrole-2-carboxaldehyde, respectively.

(1*E*,4*Z*,6*E*)-5-Hydroxy-1,7-di(pyridin-3-yl)hepta-1,4,6-trien-3-one (**2**): Yellow crystals (50%); column chromatography [EtOAc/MeOH 19:1; R_f (SiO_2) = 0.18]; m.p. 171 °C; ^{1}H NMR (400 MHz, $CDCl_3$): δ = 5.89 (1H, s), 6.71 (2H, d, J = 15.9 Hz), 7.35 (2H, dd, J = 8.0, 4.8 Hz), 7.67 (2H, d, J = 15.9 Hz), 7.87 (2H, dt, J = 8.0, 1.8 Hz), 8.61 (2H, dd, J = 4.8, 1.8H), 8.80 ppm (2H, d, J = 1.8 Hz); ^{13}C NMR (100 MHz, $CDCl_3$): δ = 102.2, 123.8, 125.8, 130.7, 134.3, 137.2, 149.8, 150.8, 182.8 ppm. IR (ATR): $\tilde{\nu}$ = 3030, 1625, 1571, 1475, 1413 cm^{-1}; MS (70 eV): m/z (%) = 279 $[M+1]^+$ (100).

(1*E*,4*Z*,6*E*)-5-Hydroxy-1,7-di(1*H*-indol-3-yl)hepta-1,4,6-trien-3-one (**3**): Dark red crystals (49%); column chromatography [EtOAc/petroleum ether 1:1; R_f (SiO_2) = 0.30]; m.p. 223 °C; ^{1}H NMR (400 MHz, [D_6]DMSO): δ = 6.41 (s, 1H), 6.72 (2H, d, J = 15.8 Hz), 7.22 (4H, qd, J = 13.8, 1.2 Hz), 7.49 (2H, dd, J = 6.9, 1.6 Hz), 7.89 (2H, d, J = 15.8 Hz), 7.96–8.00 (4H, m), 11.81 ppm (2H, s); ^{13}C NMR (100 MHz, [D_6]DMSO): δ = 100.5, 112.9, 113.2, 118.7, 120.5, 121.4, 123.1, 125.4, 132.3, 134.8, 138.0, 183.7 ppm. IR (ATR): $\tilde{\nu}$ = 3377 (br), 1607, 1572 cm^{-1}; MS (70 eV): m/z (%) = 355 $[M+1]^+$ (100).

(1*E*,4*Z*,6*E*)-5-Hydroxy-1,7-di(1*H*-pyrrol-2-yl)hepta-1,4,6-trien-3-one (**4**): Orange solid (66%); column chromatography [EtOAc/petroleum ether 1:1; R_f (SiO_2) = 0.67]; m.p. 200 °C; ^{1}H NMR (400 MHz, [D_6]DMSO): δ = 5.77 (1H, s), 6.19 (2H, br s), 6.46 (2H, d, J = 15.7 Hz), 6.60 (2H, br s), 7.06 (2H, s), 7.44 (2H, d, J = 15.7 Hz), 11.55 ppm (2H, s); ^{13}C NMR (100 MHz, [D_6]DMSO): δ = 100.4, 110.9, 115.0, 117.6, 124.2, 129.5, 130.7, 183.2 ppm; IR (ATR): $\tilde{\nu}$ = 3383 (br), 1609, 1585 cm^{-1}; MS (70 eV): m/z (%) = 255 $[M+1]^+$ (100).

Representative Procedure for the Synthesis of β-Enaminones 5a–f and Dihydropyridin-4-ones 6d and 6f

(1*E*,4*Z*,6*E*)-5-Hydroxy-1,7-di(pyridin-3-yl)hepta-1,4,6-trien-3-one (**2**; 1 mmol, 278 mg) was dissolved in 2-MeTHF (5 mL) in a 10 mL microwave tube. To this, montmorillonite clay (MK10; 556 mg, 2 equiv mass) was added as an activator. Isobutylamine (0.50 mL, 5 mmol, 5 equiv) and acetic acid (0.14 mL, 2.4 mmol, 2.4 equiv) were then added, and the mixture was stirred at 80 °C for 75 min under microwave irradiation. At the end of the reaction, the mixture was filtered over Celite, and the filter cake was thoroughly rinsed with ethanol (300 mL). The filtrate was then concentrated under reduced pressure until about 30 mL of ethanol remained. Then, ethyl acetate (300 mL) was added, and the mixture was washed with a saturated solution of sodium bicarbonate (50 mL). The aqueous phase was washed with ethyl acetate (2×30 mL). The combined organic layer was washed with water, dried (magnesium sulfate), filtered, and concentrated under reduced pressure. Column chromatography (SiO_2, EtOAc/MeOH 9:1) afforded (1*E*,4*Z*,6*E*)-5-isobutylamino-1,7-di(pyridin-3-yl)hepta-1,4,6-trien-3-one (**5a**; 79.9 mg, 24%). A similar procedure was then applied for β-enaminones **5b–f** and dihydropyridin-4-ones **6d** and **6f**. The reactions were performed by using ethanol instead of 2-MeTHF to afford the expected products. The crude products were subjected to purification by normal-phase column chromatography (SiO_2, EtOAc/MeOH 9:1) to obtain expected compounds **5b**, **5c**, and **5e**. For compounds **5d**, **5f**, **6d**, and **6f**, reverse-phase column chromatography (acetonitrile/water, gradient conditions from 10 to 100%) was used to purify to obtain the desired compounds.

(1*E*,4*Z*,6*E*)-5-Isobutylamino-1,7-di(pyridin-3-yl)hepta-1,4,6-trien-3-one (**5a**): Orange oil (24%); column chromatography [EtOAc/MeOH 19:1; R_f (SiO_2) = 0.18]; ^{1}H NMR (400 MHz, $CDCl_3$): δ = 1.05 (6H, d, J = 6.5 Hz), 1.96 (1H, nonet, J = 6.5 Hz), 3.25 (2H, ~t, J = 6.5 Hz), 5.55 (1H, s), 6.84 (1H, d, J = 15.8 Hz), 6.92 (1H, d, J = 16.1 Hz), 7.26 (1H, d, J = 16.1 Hz), 7.29 (1H, dd, J = 8.0, 4.5 Hz), 7.35 (1H, dd, J = 8.0, 4.5 Hz), 7.53 (1H, d, J = 15.8 Hz), 7.83 (2H, d, J = 8.0 Hz), 8.54 (1H, d, J = 4.5 Hz), 8.60 (1H, d, J = 4.5 Hz), 8.75–8.78 (2H, m), 11.67 ppm (1H, t, J = 6.0 Hz); ^{13}C NMR (100 MHz, $CDCl_3$): δ = 20.2, 29.4, 51.5, 94.1, 122.8, 123.6, 123.8, 130.7, 131.2, 131.7, 133.5, 133.7, 134.0, 134.1, 149.1, 149.4, 149.8, 150.3, 162.4,

184.8 ppm; IR (ATR): $\tilde{\nu}$ = 3032, 2958, 1641, 1575, 1544, 1508, 1413 cm^{-1}; MS (70 eV): *m/z* (%) = 334 $[M+1]^+$ (100).

(1*E*,4*Z*,6*E*)-5-Cyclohexylamino-1,7-di(pyridin-3-yl)hepta-1,4,6-trien-3-one (**5 b**): Yellow crystals (6%); column chromatography [EtOAc/MeOH 9:1; R_f (SiO_2) = 0.26] and recrystallization (MeOH); m.p. 174 °C; ^{1}H NMR (400 MHz, $CDCl_3$): δ = 1.30–1.65 (6H, m), 1.80–1.84 (2H, m), 1.94–1.97 (2H, m), 3.56–3.63 (1H, m), 5.52 (1H, s), 6.83 (1H, d, *J* = 15.8 Hz), 6.94 (1H, d, *J* = 15.9 Hz), 7.27 (1H, d, *J* = 15.9 Hz), 7.29 (1H, dd, *J* = 7.9, 4.8 Hz), 7.35 (1H, dd, *J* = 7.9, 4.8 Hz), 7.52 (1H, d, *J* = 15.8 Hz), 7.81–7.84 (2H, m), 8.54 (1H, dd, *J* = 4.8, 1.8 Hz), 8.60 (1H, dd, *J* = 4.8, 1.8 Hz), 8.75 (1H, d, *J* = 1.8 Hz), 8.77 (1H, d, *J* = 1.8 Hz), 11.71 ppm (1H, d, *J* = 8.1 Hz); ^{13}C NMR (100 MHz, $CDCl_3$): δ = 24.2, 25.3, 33.8, 52.2, 93.9, 122.7, 123.6, 123.8, 130.7, 131.3, 131.8, 133.4, 133.7, 133.9, 134.1, 149.1, 149.4, 149.8, 150.3, 161.1, 184.6 ppm; IR (ATR): $\tilde{\nu}$ = 3361 (br), 2929, 1633, 1571, 1510, 1415 cm^{-1}; MS (70 eV): *m/z* (%) = 360 $[M+1]^+$ (100).

(1*E*,4*Z*,6*E*)-5-(2-Methoxyethylamino)-1,7-di(pyridin-3-yl)hepta-1,4,6-trien-3-one (**5 c**): Orange-red viscous oil (16%); column chromatography [EtOAc/MeOH 9:1; R_f (SiO_2) = 0.12]; ^{1}H NMR (400 MHz, $CDCl_3$): δ = 3.43 (3H, s), 3.60–3.61 (4H, m), 5.57 (1H, s), 6.84 (1H, d, *J* = 15.8 Hz), 7.02 (1H, d, *J* = 16.1 Hz), 7.24 (1H, d, *J* = 16.1 Hz), 7.30 (1H, dd, *J* = 7.9, 4.8 Hz), 7.34 (1H, dd, *J* = 7.9, 4.8 Hz), 7.53 (1H, d, *J* = 15.8 Hz), 7.81–7.85 (2H, m), 8.54 (1H, dd, *J* = 4.8, 1.9 Hz), 8.60 (1H, dd, *J* = 4.8, 1.9 Hz), 8.74 (1H, d, *J* = 1.9 Hz), 8.78 (1H, d, *J* = 1.9 Hz), 11.55 ppm (1H, br s); ^{13}C NMR (100 MHz, $CDCl_3$): δ = 43.8, 59.3, 71.7, 94.4, 123.2, 123.6, 123.7, 130.6, 131.3, 131.7, 133.7, 133.8, 133.9, 134.1, 149.2, 149.5, 149.8, 150.3, 162.5, 185.2 ppm; IR (ATR): $\tilde{\nu}$ = 3053, 2922, 1645, 1568, 1506, 1425, 1411 cm^{-1}; MS (70 eV): *m/z* (%) = 336 $[M+1]^+$ (100).

(1*E*,4*Z*,6*E*)-5-(3-Methoxypropylamino)-1,7-di(pyridin-3-yl)hepta-1,4,6-trien-3-one (**5 d**): Orange oil (4%); normal-phase column chromatography [EtOAc/MeOH 9:1; R_f (SiO_2) = 0.13] and reverse-phase column chromatography (CH_3CN/H_2O 30:70 to 100:0), ^{1}H NMR (400 MHz, $CDCl_3$): δ = 1.93 (2H, quint, *J* = 6.0 Hz), 3.36 (3H, s), 3.50 (2H, t, *J* = 6.0 Hz), 3.55 (2H, q, *J* = 6.0 Hz), 5.57 (1H, s), 6.84 (1H, d, *J* = 15.8 Hz), 7.01 (1H, d, *J* = 16.2 Hz), 7.27 (1H, d, *J* = 16.2 Hz), 7.30 (1H, dd, *J* = 7.9, 4.8 Hz), 7.35 (1H, dd, *J* = 8.1, 4.8 Hz), 7.52 (1H, d, *J* = 15.8 Hz), 7.82–7.86 (2H, m), 8.54 (1H, dd, *J* = 4.8, 1.5 Hz), 8.60 (1H, dd, *J* = 4.8, 1.5 Hz), 8.75 (1H, d, *J* = 1.5 Hz), 8.78 (1H, d, *J* = 1.5 Hz), 11.55 ppm (1H, t, *J* = 6.0 Hz); ^{13}C NMR (100 MHz, $CDCl_3$): δ = 30.5, 40.6, 58.8, 69.0, 93.9, 122.7, 123.6, 123.7, 130.7, 131.2, 131.7, 133.57, 133.64, 134.0, 134.1, 149.3, 149.5, 149.8, 150.3, 162.5, 184.9 ppm; IR (ATR): $\tilde{\nu}$ = 3226 (br), 3032, 2929, 1710, 1639, 1566, 1512, 1413 cm^{-1}; MS (70 eV): *m/z* (%) = 350 $[M+1]^+$ (100).

(1*E*,4*Z*,6*E*)-5-(2-Hydroxyethylamino)-1,7-di(pyridin-3-yl)hepta-1,4,6-trien-3-one (**5 e**): Red-brown crystals (12%); column chromatography [EtOAc/MeOH 9:1; R_f (SiO_2) = 0.05]; m.p. 83 °C; ^{1}H NMR (400 MHz, $CDCl_3$): δ = 3.61 (2H, q, *J* = 5.4 Hz), 3.88 (2H, t, *J* = 5,4 Hz), 5.59 (1H, s), 6.83 (1H, d, *J* = 15.9 Hz), 7.03 (1H, d, *J* = 16.2 Hz), 7.26 (1H, d, *J* = 16.2 Hz), 7.30 (1H, dd, *J* = 7.8, 4.8 Hz), 7.34 (1H, dd, *J* = 7.7, 4.8 Hz), 7.52 (1H, d, *J* = 15.9 Hz), 7.82–7.85 (2H, m), 8.54 (1H, dd, *J* = 4.8, 1.6 Hz), 8.59 (1H, dd, *J* = 4.8, 1.6 Hz), 8.74 (1H, d, *J* = 1.6 Hz), 8.77 (1H, d, *J* = 1.6 Hz), 11.61 ppm (1H, t, *J* = 5.4 Hz); ^{13}C NMR (100 MHz, $CDCl_3$): δ = 45.9, 62.1, 94.6, 123.0, 123,6, 123.8, 130.5, 131.1, 131.6, 133.7, 133.9, 134.1, 134.2, 149.2, 149.4, 149.8, 150.4, 162.8, 185.3 ppm; IR (ATR): $\tilde{\nu}$ = 3292 (br), 3045, 2927, 1672, 1641, 1568, 1510, 1490, 1413 cm^{-1}; MS (70 eV): *m/z* (%) = 322 $[M+1]^+$ (100).

(1*E*,4*Z*,6*E*)-5-(3-Hydroxypropylamino)-1,7-di(pyridin-3-yl)hepta-1,4,6-trien-3-one (**5 f**): Dark-brown oil (16%); reverse-phase chromatography, t_R = 2.93 min (gradient conditions, 10% acetonitrile in water to 100% acetonitrile, 5 min, flow rate: 1 mL min^{-1}); ^{1}H NMR (400 MHz, [D_4]methanol): δ = 1.91 (2H, quint, *J* = 6.4 Hz), 3.67 (2H, t, *J* = 6.8 Hz), 3.73 (2H, t, *J* = 6.0 Hz), 5.80 (1H, s), 7.04 (1H, d, *J* = 16.0 Hz), 7.33 (1H, d, *J* = 16.2 Hz), 7.44 −7.54 (4H, m), 8.10 (1H, dt, *J* = 7.9 and 1.6 Hz), 8.20 (1H, dt, *J* = 7.7, 1.8 Hz), 8.11 (1H, d, *J* = 8.0 Hz), 8.20 (1H, d, *J* = 8.0 Hz), 8.74 (1H, d, *J* = 1.5 Hz), 8.80 ppm (1H, s); ^{13}C NMR (100 MHz, [D_4]methanol): δ = 32.7, 39.9, 58.2, 93.4, 122.6, 124.1, 124.2, 131.4, 132.1, 132.4, 132.5, 134.6, 134.66, 134.72, 148.3, 148.5, 148.7, 149.2, 163.6, 184.6 ppm; IR (ATR): $\tilde{\nu}$ = 3309 (br), 2937, 1641, 1577, 1531, 1417 cm^{-1}; MS (70 eV): *m/z* (%) = 336 $[M+1]^+$ (100).

(*E*)-1-(3-Methoxypropyl)-2-(pyridin-3-yl)-6-[2-(pyridin-3-yl)vinyl]-2,3-dihydropyridin-4(1*H*)-one (**6 d**): Brown oil (16%); reverse-phase chromatography, t_R = 0.54 min (30% acetonitrile in water to 100% acetonitrile, 5 min, flow rate: 1 mL min^{-1}); ^{1}H NMR (400 MHz, [D_4]methanol): δ = 1.93–1.96 (2H, m), 2.60 (1H, d, *J* = 16.8 Hz), 3.30 (3H, s), 3.26–3.34 (2H, m,), 3.44–3.48 (2H, m), 4.04–4.11 (1H, m), 5.11 (1H, dd, *J* = 7.6, 1.6 Hz), 5.42 (1H, s), 7.44–7.54 (4H, m), 7.85 (1H, d, *J* = 7.9 Hz), 8.18 (1H, d, *J* = 7.9 Hz), 8.51 (1H, d, *J* = 4.4 Hz), 8.54 (2H, br s), 8.81 ppm (1H, s); ^{13}C NMR (100 MHz, [D_4]methanol): δ = 30.6, 42.5, 49.4, 58.9, 60.2, 70.0, 98.0, 125.4, 125.6, 133.5, 136.3, 136.37, 136.39, 136.6, 148.5, 149.6, 149.8, 150.6, 164.1, 191.6 ppm; IR (ATR): $\tilde{\nu}$ = 2926, 1620 1531, 1479, 1421 cm^{-1}; MS (70 eV): *m/z* (%) = 350 $[M+1]^+$ (100).

(*E*)-1-(3-Hydroxypropyl)-2-(pyridin-3-yl)-6-[2-(pyridin-3-yl)vinyl]-2,3-dihydropyridin-4(1*H*)-one (**6 f**): Dark-orange oil (7%); reverse-phase chromatography, t_R = 2.62 min (gradient conditions, 10% acetonitrile in water to 100% acetonitrile, 5 min, flow rate: 1 mL min^{-1}); ^{1}H NMR (400 MHz, [D_4]methanol): δ = 1.84–1.94 (2H, m), 2.58 (1H, d, *J* = 16.8 Hz), 3.25–3.38 (2H, m), 3.63 (2H, t, *J* = 5.6 Hz), 4.00–4.10 (1H, quint, *J* = 7.2 Hz), 5.13 (1H, dd, *J* = 7.8, 2.1 Hz), 5.40 (1H, s), 7.43–7.51 (4H, m), 7.84 (1H, dt, *J* = 8.0, 2.0 Hz), 8.49 (1H, dt, *J* = 8.0, 2.0 Hz), 8.50 (1H, dd, *J* = 4.8, 0.8 Hz), 8.51 (1H, d, *J* = 1.1 Hz), 8.53 (1H, d, *J* = 1.3 Hz), 8.80 ppm (1H, d, *J* = 1.6 Hz); ^{13}C NMR (100 MHz, [D_4]methanol): δ = 33.2, 42.5, 49.4, 59.3, 60.4, 98.1, 125.4, 125.5, 133.5, 136.3, 136.5, 136.6, 148.5, 149.6, 149.9, 150.6, 164.2, 191.5 ppm; IR (ATR): $\tilde{\nu}$ = 3265 (br), 1591, 1517, 1492, 1415 cm^{-1}; MS (70 eV): *m/z* (%) = 336 $[M+1]^+$ (100).

Biological Studies

General

MEM nonessential amino acid solution (NEAA), 2,2-diphenyl-1-picrylhydrazyl (DPPH), penicillin/streptomycin (P/S), Trolox, and 2,7-dichlorofluorescein diacetate were purchased from Sigma–Aldrich, whereas 3-(4,5-dimethylthiazol-2-yl)-2,5-diphenyltetrazolium bromide (MTT) and trypan blue were obtained from Amresco. Trypsin/ethylenediaminetetraacetic acid (EDTA) solution and Dulbecco's phosphate-buffered saline (PBS^-, no calcium and no magnesium) were obtained from Life Technologies, and fetal bovine serum (FBS) was obtained from Greiner Bio-one. All cell lines, Caco-2 (colorectal adenocarcinoma), HepG2 (hepatocellular carcinoma), CHO (Chinese hamster ovary), HT-29 (colorectal adenocarcinoma), and EA.hy926 (endothelial), were obtained from ATCC. These cell lines were cultivated and maintained in a growth medium containing Dulbecco's modified Eagle medium (DMEM) + glutamax, 1% NEAA, 1% P/S, and 10% FBS. During the MTT experiment, serum-free medium was used to avoid interferences. Each compound or positive control was dissolved in DMSO to prepare the 25 mM stock solution for both cytotoxicity and antioxidant tests. The stock solu-

tions were aliquoted and stored in a refrigerator for the further replicate experiment.

Cytotoxicity Activity: MTT Experiments

Throughout the experiment, standard procedures were used to maintain all cell lines at 37 °C with 95% humidity and 10% CO_2. Using adherent cells, the MTT assay was performed to determine the number of viable cells in this assay. Briefly, 2×10^4 cells suspended in DMEM (200 μL) were first inoculated into each well of a 96-well microplate and were incubated for 24 h. Then, the medium in each well was removed and an equal volume of serum-free medium (200 μL well^{-1}) containing either test compound or positive control (doxorubicin hydrochloride, DOX) at various concentrations was added for 72 h. Each compound was performed in triplicate. Afterwards, the cell viability was determined by removing 100 μL of medium and adding 20 μL of MTT solution (5 mg mL^{-1} in PBS) followed by 2 h of incubation. Finally, DMEM with MTT solution was then removed and replaced with DMSO to dissolve the formazan crystal. The 96-well microplate was then measured at $\lambda=$ 570 nm by using a Spectramax (Molecular Devices) microplate spectrophotometer. For data analysis, the percentage of surviving cells after exposure to various concentrations of each test compound for 72 h was calculated to obtain the IC_{50} value of each compound.

Protein Content (SRB) Analysis

The SRB assay is based on the measurement of cellular proteins. Sulforhodamine B can bind electrostatically with basic amino acid residues if the cells are fixed with trichloroacetic acid (TCA) and can be solubilized by weak bases. Because of this quantitative staining capacity of SRB, the assay is used to screen for cytotoxicity and cell density. The cells were seeded at a concentration of 2×10^4 cells per well for 24 h and were treated with or without (control) compounds. Three days after this treatment, the cells were fixed by adding 50% TCA in Milli-Q water (50 μL) for 1 h in the cold room, 4 °C. The plate was washed at least three times with tap water and was then dried, after which the cells were stained with SRB solution (0.4% sulforhodamine B in 1% glacial acetic acid) at 4 °C. After 30 min, the plate was rinsed with 1% glacial acetic acid (5×) dried. Sequentially, Tris buffer in a concentration of 10 mM was used to redissolve the stain. Finally, the absorbance was measured using the microplate spectrophotometer at a wavelength of 490 nm. Each condition was performed in triplicate.

Reactive Oxygen Species (ROS) Assay

The experiments were performed in an incubator at 37 °C with 10% CO_2. Seeding of a concentration of 2×10^4 cells per well in DMEM was performed in a black 96-well plate with transparent bottom. After 24 h, the confluent cells were equally treated with or without the compounds at 10 and 1 μM in serum-free medium (200 μL). Then, after removal of the medium, the cells were washed with PBS buffer followed by the addition of 2,7-dichlorofluorescein diacetate (DCFH-DA, 20 μM) for a 30 min incubation period. Thereafter, DCFH-DA was removed, and the cells were washed with PBS. Afterwards, DMEM without phenol red medium was added in equal volume for 1 h of incubation. Finally, the black 96-well plates were measured for fluorescence with a Gemini XPS Microplate Reader with an excitation of $\lambda=$485 nm and an emission of $\lambda=$535 nm. Afterwards, the plate experiments were continued to evaluate the protein content with a similar protocol as for the SRB assay described above. The SRB assay was used to normalize the results, which were related to the amount of protein present in each well.

Chemical Antioxidant Capacity: DPPH Scavenger

The 1,1-diphenyl-2-picrylhydrazyl (DPPH) radical is commonly used to determine antioxidant activity. First, DPPH was freshly prepared at 5 mg mL^{-1} in DMSO. Then, DPPH was diluted into 200 μM in MeOH for antioxidant measurements. In addition, stock solutions of test compounds were also properly diluted in MeOH at various concentrations. Afterwards, 200 μM DPPH solution (100 μL) was then added into 96-well microplates. Subsequently, test compound (100 μL) at various concentrations and blanks without derivative were individually added into each well and vigorously mixed for 30 min in the dark chamber at 30 °C. After incubation in darkness, the solutions were measured at $\lambda=$515 nm by using a Spectramax microplate spectrophotometer. The required concentration to reduce the absorbance by 50% (EC_{50}) was calculated from the equation obtained by fitting the linear part of the absorption curves. A positive compound, namely, Trolox, was used as reference. The results are the mean values determined from at least three independent experiments for each compound [Eq. (1)]:

$$I\,[\%] = \frac{[\mathrm{AbsB}-(\mathrm{AbsS}-\mathrm{AbsSC})]}{\mathrm{AbsB}} \times 100 \qquad (1)$$

in which I [%] is the percentage of inhibition at various concentrations, AbsB is the absorption of blank DPPH in MeOH, AbsS is the absorption of sample with DPPH at various concentrations, and AbsSC is absorption of sample control without DPPH at various concentrations.

Ferric Reducing Ability of Plasma (FRAP) Assay

An acetate buffer of 300 mM was prepared by adding sodium acetate trihydrate (3.1 g) to acetic acid (16 mL) and was diluted to 1000 mL with Milli-Q water. A TPTZ (2,4,6-tripyridyl-*s*-triazine) solution of 10 mM was prepared by adding TPTZ (0.156 g) to ethanol (50 mL). Lastly, a 20 mM solution of iron(III) chloride hexahydrate was prepared by mixing $FeCl_3{\cdot}6H_2O$ (0.5404 g) with 37% HCl (2 mL) and Milli-Q water (98 mL). The TPTZ and iron solutions were freshly prepared on the day of the assay. These three mixtures were added in a 10:1:1 ratio to obtain the FRAP reagent. Finally, samples (100 μL) were mixed with the FRAP reagent (900 μL) and after 4 min the absorbance was measured at $\lambda=$593 nm with a Spectramax microplate spectrophotometer. Trolox was used as a standard, and the FRAP value was calculated as Trolox equivalent [μM] through linear regression of the Trolox standard curve.

Water Solubility and Stability Measurements

The shake flask method is commonly used to measure aqueous solubility.[12] The test compounds were first measured for maximum absorbance by using the liquid chromatography (LC) technique using Ascentis Express C18, HPLC column 3 cm×4.6 mm, 2.7 μm (LC method for 5 min at flow rate 1 mL min^{-1} during the gradient elution). Afterwards, the standard curves were prepared from various concentrations of the test compounds. In this experiment, a sodium phosphate buffered solution at pH 6.8 was used to perform the solubility test of each β-enaminone compound. An excess amount of a solid compound was added into 1 mL of the phos-

phate-buffered solution (pH 6.8). The experiment was divided into two time points. The first one was fixed at 90 min under a sonicator bath at 37 °C and the second one at 30 min under a sonicator bath at 37 °C followed by 23 h of incubation at 300 rpm and sonication for another 30 min. Both time points of each sample were centrifuged at 14000 rpm for 5 min. Then, all compounds were filtered (0.2 μm) at 37 °C. Subsequently, the solutions were diluted in DMSO to avoid precipitation of the compounds at room temperature. Each compound was individually measured at its maximum absorbance. Finally, the solubility values were calculated from the linear equations of each standard curve. The experiment was independently triplicated.

Acknowledgements

The authors are indebted to Ghent University and to the Lotus+ Erasmus Mundus Programme of the European Union for financial support.

Conflict of Interest

The authors declare no conflict of interest.

Keywords: biological activity · cytotoxicity · enaminones · nitrogen heterocycles · oxidative stress

[1] H. J. J. Pabon, *Rec. Trav. Chim. Pays Bas* **1964**, *83*, 379–386.
[2] a) U. Pedersen, P. B. Rasmussen, S.-O. Lawesson, *Liebigs Ann. Chem.* **1985**, *1985*, 1557–1569; b) M. A. Khan, R. El-Khatib, K. D. Rainsford, M. W. Whitehouse, *Bioorg. Chem.* **2012**, *40*, 30–38; c) V. D. John, M. B. Ummathur, K. Krishnankutty, *J. Coord. Chem.* **2013**, *66*, 1508–1518.
[3] a) R. Hanif, L. Qiao, S. J. Shiff, B. Rigas, *J. Lab. Clin. Med.* **1997**, *130*, 576–584; b) K. Mehta, P. Pantazis, T. McQueen, B. B. Aggarwal, *Anti-cancer Drugs* **1997**, *8*, 470–481; c) T. M. Elattar, A. S. Virji, *Anticancer Res.* **2000**, *20*, 1733–1738; d) A. Mukhopadhyay, C. Bueso-Ramos, D. Chatterjee, P. Pantazis, B. B. Aggarwal, *Oncogene* **2001**, *20*, 7597–7609; e) D. R. Siwak, S. Shishodia, B. B. Aggarwal, R. Kurzrock, *Cancer* **2005**, *104*, 879–890; f) Y. G. Lin, A. B. Kunnumakkara, A. Nair, W. M. Merritt, L. Y. Han, G. N. Armaiz-Pena, A. A. Kamat, W. A. Spannuth, D. M. Gershenson, S. K. Lutgendorf, B. B. Aggarwal, A. K. Sood, *Clin. Cancer Res.* **2007**, *13*, 3423–3430.
[4] a) S. D. Deodhar, R. Sethi, R. C. Srimal, *Indian J. Med. Res.* **1980**, *71*, 632–634; b) M. A. Azuine, S. V. Bhide, *Nutr. Cancer* **1992**, *17*, 77–83; c) G. Shoba, D. Joy, T. Joseph, M. Majeed, R. Rajendran, P. S. Srinivas, *Planta Med.* **1998**, *64*, 353–356; d) A. L. Cheng, C. H. Hsu, J. K. Lin, M. M. Hsu, Y. F. Ho, T. S. Shen, J. Y. Ko, J. T. Lin, B. R. Lin, W. Ming-Shiang, H. S. Yu, S. H. Jee, G. S. Chen, T. M. Chen, C. A. Chen, M. K. Lai, Y. S. Pu, M. H. Pan, Y. J. Wang, C. C. Tsai, C. Y. Hsieh, *Anticancer Res.* **2001**, *21*, 2895–2900; e) C. D. Lao, M. T. t. Ruffin, D. Normolle, D. D. Heath, S. I. Murray, J. M. Bailey, M. E. Boggs, J. Crowell, C. L. Rock, D. E. Brenner, *BMC Complementary Altern. Med.* **2006**, *6*, 10.
[5] a) V. Ravindranath, N. Chandrasekhara, *Toxicology* **1981**, *22*, 337–344; b) R. A. Sharma, H. R. McLelland, K. A. Hill, C. R. Ireson, S. A. Euden, M. M. Manson, M. Pirmohamed, L. J. Marnett, A. J. Gescher, W. P. Steward, *Clin. Cancer Res.* **2001**, *7*, 1894–1900; c) G. Garcea, D. J. L. Jones, R. Singh, A. R. Dennison, P. B. Farmer, R. A. Sharma, W. P. Steward, A. J. Gescher, D. P. Berry, *Br. J. Cancer* **2004**, *90*, 1011–1015; d) P. Anand, A. B. Kunnumakkara, R. A. Newman, B. B. Aggarwal, *Mol. Pharm.* **2007**, *4*, 807–818; e) K. M. Nelson, J. L. Dahlin, J. Bisson, J. Graham, G. F. Pauli, M. A. Walters, *J. Med. Chem.* **2017**, *60*, 1620–1637.
[6] a) A. R. Reddy, P. Dinesh, A. S. Prabhakar, K. Umasankar, B. Shireesha, M. B. Raju, *Mini-Rev. Med. Chem.* **2013**, *13*, 1769–1777; b) A. Vyas, P. Dandawate, S. Padhye, A. Ahmad, F. Sarkar, *Curr. Pharm. Des.* **2013**, *19*, 2047–2069.
[7] a) R. De Vreese, C. Grootaert, S. D'hoore, A. Theppawong, S. Van Damme, M. Van Bogaert, J. Van Camp, M. D'hooghe, *Eur. J. Med. Chem.* **2016**, *123*, 727–736; b) A. Theppawong, R. De Vreese, L. Vannecke, C. Grootaert, J. Van Camp, M. D'hooghe, *Bioorg. Med. Chem. Lett.* **2016**, *26*, 5650–5656.
[8] J. A. Makawana, M. P. Patel, R. G. Patel, *Chin. Chem. Lett.* **2012**, *23*, 427–430.
[9] J. E. Foster, J. M. Nicholson, R. Butcher, J. P. Stables, I. O. Edafiogho, A. M. Goodwin, M. C. Henson, C. A. Smith, K. R. Scott, *Bioorg. Med. Chem.* **1999**, *7*, 2415–2425.
[10] D. Simoni, M. Rizzi, R. Rondanin, R. Baruchello, P. Marchetti, F. P. Invidiata, M. Labbozzetta, P. Poma, V. Carina, M. Notarbartolo, A. Alaimo, N. D'Alessandro, *Bioorg. Med. Chem. Lett.* **2008**, *18*, 845–849.
[11] a) Y. Liu, M. Ye, Q. Wu, L. Wu, J. Xu, *Lett. Drug Des. Discovery* **2014**, *11*, 993–999; b) S. Raghavan, P. Manogaran, K. K. Gadepalli Narasimha, B. Kalpattu Kuppusami, P. Mariyappan, A. Gopalakrishnan, G. Venkatraman, *Bioorg. Med. Chem. Lett.* **2015**, *25*, 3601–3605.
[12] a) L. Zhou, L. Yang, S. Tilton, J. Wang, *J. Pharm. Sci.* **2007**, *96*, 3052–3071; b) E. Baka, J. E. Comer, K. Takacs-Novak, *J. Pharm. Biomed. Anal.* **2008**, *46*, 335–341.
[13] a) I. F. F. Benzie, J. J. Strain, *Anal. Biochem.* **1996**, *239*, 70–76; b) G. Litwinienko, K. U. Ingold, *J. Org. Chem.* **2004**, *69*, 5888–5896; c) K. Thaipong, U. Boonprakob, K. Crosby, L. Cisneros-Zevallos, D. Hawkins Byrne, *J. Food Compos. Anal.* **2006**, *19*, 669–675; d) K. Mishra, H. Ojha, N. K. Chaudhury, *Food Chem.* **2012**, *130*, 1036–1043.
[14] a) D. Karunagaran, R. Rashmi, T. R. Kumar, *Curr. Cancer Drug Targets* **2005**, *5*, 117–129; b) J. J. Johnson, H. Mukhtar, *Cancer Lett.* **2007**, *255*, 170–181; c) A. B. Kunnumakkara, P. Anand, B. B. Aggarwal, *Cancer Lett.* **2008**, *269*, 199–225.
[15] P. Sanz, O. Mó, M. Yáñez, J. Elguero, *J. Phys. Chem. A* **2007**, *111*, 3585–3591.
[16] P. Steer, J. Millgard, D. M. Sarabi, S. Basu, B. Vessby, T. Kahan, M. Edner, L. Lind, *Lipids* **2002**, *37*, 231–236.
[17] G. Waris, H. Ahsan, *J. Carcinog.* **2006**, *5*, 14–14.
[18] M. L. Circu, T. Y. Aw, *Free Radical Biol. Med.* **2010**, *48*, 749–762.
[19] V. Di Matteo, E. Esposito, *Curr. Drug Targets: CNS Neurol. Disord.* **2003**, *2*, 95–107.
[20] R. Angelopoulou, G. Lavranos, P. Manolakou, *Reprod. Toxicol.* **2009**, *28*, 167–171.
[21] M. Valko, D. Leibfritz, J. Moncol, M. T. Cronin, M. Mazur, J. Telser, *Int. J. Biochem. Cell Biol.* **2007**, *39*, 44–84.
[22] M. Gerber, M. C. Boutron-Ruault, S. Hercberg, E. Riboli, A. Scalbert, M. H. Siess, *Bull. Cancer* **2002**, *89*, 293–312.
[23] T. Atsumi, K. Tonosaki, S. Fujisawa, *Arch. Oral Biol.* **2006**, *51*, 913–921.
[24] R. Jäger, R. P. Lowery, A. V. Calvanese, J. M. Joy, M. Purpura, J. M. Wilson, *Nutr. J.* **2014**, *13*, 11.
[25] a) S.-Y. Sun, *Cancer Biol. Ther.* **2010**, *9*, 109–110; b) M. Halasi, M. Wang, T. S. Chavan, V. Gaponenko, N. Hay, A. L. Gartel, *Biochem. J.* **2013**, *454*, 201–208.
[26] a) T. Atsumi, K. Tonosaki, S. Fujisawa, *Anticancer Res.* **2007**, *27*, 363–371; b) F. Thayyullathil, S. Chathoth, A. Hago, M. Patel, S. Galadari, *Free Radical Biol. Med.* **2008**, *45*, 1403–1412; c) Y. Sanchez, G. P. Simon, E. Calvino, E. de Blas, P. Aller, *J. Pharmacol. Exp. Ther.* **2010**, *335*, 114–123; d) M. B. Chen, X. Y. Wu, G. Q. Tao, C. Y. Liu, J. Chen, L. Q. Wang, P. H. Lu, *Int. J. Cancer* **2012**, *131*, 2487–2498; e) S. U. Gandhy, K. Kim, L. Larsen, R. J. Rosengren, S. Safe, *BMC cancer* **2012**, *12*, 564; f) G. D. Noratto, I. Jutooru, S. Safe, G. Angel-Morales, S. U. Mertens-Talcott, *Mol. Nutr. Food Res.* **2013**, *57*, 1638–1648; g) D. Wang, J. Hu, L. Lv, X. Xia, J. Liu, X. Li, *Oncol. Lett.* **2013**, *6*, 81–85; h) X. Zhang, M. Chen, P. Zou, K. Kanchana, Q. Weng, W. Chen, P. Zhong, J. Ji, H. Zhou, L. He, G. Liang, *BMC cancer* **2015**, *15*, 866.
[27] S. J. Duthie, W. T. Melvin, M. D. Burke, *Xenobiotica* **1994**, *24*, 265–279.
[28] H. Abdi, L. J. Williams, *Wiley Interdiscip. Rev. Comput. Stat.* **2010**, *2*, 433–459.
[29] W. N. Dudley, J. G. Benuzillo, M. S. Carrico, *Nurs. Res.* **2004**, *53*, 59–62.
[30] H. Yu, Q. Huang, *J. Agric. Food Chem.* **2011**, *59*, 9120–9126.
[31] a) G. Williamson, A. J. Day, G. W. Plumb, D. Couteau, *Biochem. Soc. Trans.* **2000**, *28*, 16–22; b) Y. Konishi, S. Kobayashi, M. Shimizu, *J. Agric. Food Chem.* **2003**, *51*, 7296–7302; c) S. Gao, M. Hu, *Mini-Rev. Med. Chem.* **2010**, *10*, 550–567; d) S. Manzano, G. Williamson, *Mol. Nutr. Food Res.* **2010**, *54*, 1773–1780; e) G. R. Velderrain-Rodriguez, H. Palafox-Carlos, A.

Wall-Medrano, J. F. Ayala-Zavala, C. Y. O. Chen, M. Robles-Sanchez, H. Astiazaran-Garcia, E. Alvarez-Parrilla, G. A. Gonzalez-Aguilar, *Food Funct.* **2014**, *5*, 189 – 197.

[32] A. M. Calcagno, J. A. Ludwig, J. M. Fostel, M. M. Gottesman, S. V. Ambudkar, *Mol. Pharm.* **2006**, *3*, 87 – 93.

Received: February 27, 2018

